

Sphere-like Hierarchical Y Zeolite Fabricated by Steam-assisted Conversion Method

DU Yan-Ze^{1,2}, YANG Xiao-Na¹, NING Wei-Wei¹, KONG Qing-Lan¹,
QIN Bo², ZHENG Jia-Jun¹, LI Wen-Lin, LI Rui-Feng¹

(1. Key Laboratory of Coal Science and Technology MOE, Research Centre of Energy Chemical & Catalytic Technology, Taiyuan University of Technology, Taiyuan 030024, China; 2. Dalian Research Institute of Petroleum & Petrochemicals, SINOPEC, Dalian 116045, China)

Abstract: Sphere-like hierarchical Y zeolite was synthesized by a “steam-assisted conversion (SAC)” procedure. The as-synthesized samples were characterized by X-ray diffraction (XRD), scanning electron microscopy (SEM), transmission electron microscopy (TEM), N₂ adsorption-desorption, solid-state nuclear magnetic resonance (NMR) spectra, and Fourier transform infrared (IR) spectroscopy. Results observed by SEM displayed that the as-synthesized Y zeolite was sphere-like polycrystalline aggregates composed of primary crystals with size of about 50-300 nm. These results exhibited that some polycrystalline aggregates were hollow Y zeolite spheres. Combined with characterization results of FT-IR, ²⁹Si NMR, SEM, and TEM, a mechanism illustrating formation of the hollow Y zeolite polycrystalline spheres was proposed.

Key words: hierarchical; polycrystalline aggregates; hollow sphere; steam-assisted conversion

Nowadays, compare to light crude oils, the production of heavy and extra-heavy crude oils is increasing^[1]. Motors fueled with current petrol extracted from those crude oils produce more pollutants, which do much harm to people and environment. Besides difficult to be extracted and transported, heavy-oil resources are gradually difficult to be refined^[2]. Y zeolite is the main activity component used in fluid catalytic cracking (FCC) process, the most important refinery technologies to convert atmospheric and vacuum residues into fractions of motor fuels. The challenge in this process is both heavy oil and extra-heavy oil molecules are much larger than the inherent micropore channels in Y zeolite. As a consequence, most of acid centers existing in the micropores of the catalyst are inaccessible, and can not be efficiently utilized by the reactant molecules. In the past decades, it costs researchers plenty of time to prepare hierarchical zeolite^[3-9] with significantly shortened micropore channels, dramatically increased external surface area, and proliferated pore windows by introducing a complex meso- or/and macropore structure^[10-12] *via* non-templating^[6-9] and templating^[3-5] approaches to overcome these challenges.

Dealumination^[13] by steaming or/and by acid leaching, or desilication^[7] by alkaline etching, or sequential desilication-dealumination, or high energy ion irradiation-

induced ordered macropores^[9] as a representative non-templating method, involves post-etching of intact zeolites to achieve mesoporosity resulted from a partial collapse of the zeolite framework caused by the extraction of Al or Si from the zeolite framework positions. In the templating method, various template agents such as carbon black or carbon nanotubes (CTNs)^[14], surfactants^[4-5], polymers^[15] and even inorganic nanoparticles^[16] are often reported to be introduced into the zeolite crystals during synthesis, with the subsequent removal of the templates to produce mesopores^[4-5,14-16] or macropores^[16].

Besides these methods, “steam-assisted conversion (SAC)” procedure^[7-8] may be a potential and efficient approach to fabricate hierarchical zeolite materials. SAC method is also mentioned as vapour-phase method^[17] or dried gel conversion^[18-19], or steam-assisted crystallization^[20-21]. In SAC procedure, the bulk- or powder-like dried gel usually containing organic templates is separated from and out of touch with the liquid but crystallizes with the help of the vapor yielded from the liquid under autogenous pressure in the same reactor. Recently SAC method has caught much attention, because it not only dramatically cuts down the dosage of organic template^[8] but also is often adopted to prepare zeolite membranes^[21-22] or hierarchical zeolite^[7-8]. Very recently,

Received date: 2018-08-13; Modified date: 2018-09-23

Foundation item: National Natural Science Foundation of China (U1463209, 21371129, 21376157); Sino Petroleum Corp (116050)

Biography: DU Yan-Ze (1976-), male, candidate of PhD. E-mail: duyanze.fshy@sinopec.com

Corresponding author: ZHENG Jia-Jun, professor. E-mail: zhengjiacun@tyut.edu.cn

Dou, *et al.*^[7] reported that a hierarchical zeolite beta was synthesized without any seeds or secondary mesopore by SAC method. Möller, *et al.*^[8] also reported that a hierarchical mesoporous network of beta zeolite with very high micropore as well as mesopore volume was synthesized without a porogen by a dense-gel synthesis using SAC to stimulate a burst of nucleation.

However, up to now, no report has approached the synthesis of sphere-like hierarchical Y zeolite consisting of primary nanosized FAU zeolite crystals. In the present work, dried gel, the precursors yielding Y, was subjected to a vapor treatment, and sphere-like hierarchical Y zeolite aggregate was therefore synthesized by SAC procedure without assistance of any organic templates or secondary mesopore. The effects of chemical composition like $\text{SiO}_2/\text{Al}_2\text{O}_3$ in gel precursor on the formation of the sphere-like hierarchical Y zeolite were investigated and discussed in details; formation mechanism of the sphere-like hierarchical Y including hollow sphere-like Y zeolite polycrystalline aggregates was proposed on base of the results of FT-IR, ^{29}Si NMR, SEM and TEM.

1 Experimental

1.1 Synthesis

Precursor solution yielding Y zeolite was prepared with a mole composition as following: $3.53\text{Na}_2\text{O} : (4.14-8.28)\text{SiO}_2 : 1\text{Al}_2\text{O}_3 : (212-239)\text{H}_2\text{O}$. Typically, by mixing 10.2 g NaAlO_2 , 8.0 g NaOH, and 88 mL H_2O , and stirring for giving a clear solution. Then 16–32 mL colloidal silica was added into the solution followed by stirring for 2 h. The achieved Sol-Gel mixture was divided into two parts, and marked as “A” and “B”, respectively.

The synthesis of hierarchical Y zeolite was as following: the corresponding gel “A” was transferred into a polytetrafluoroethylene cup and kept at 60°C for 24 h for giving a dried gel, and the obtained dried gel was named as YP-*x*, here, “*x*” stands for $\text{SiO}_2/\text{Al}_2\text{O}_3$ ratio. 2 g of the abovementioned YP-*x* was added to a 50 mL polytetrafluoroethylene cup, and the cup was put into an autoclave without any additional water or other solvent for crystallization at 90°C for 24 h. The final product was collected by washing to neutral with water, drying in air at 110°C , and denoted as YS-*x*.

Y zeolite prepared by a traditional hydrothermal procedure was described as following: the corresponding gel “B” was transferred into an autoclave and kept at 90°C for 24 h under autogenous pressure. The product was collected by filtration, washed with distilled water, dried in air, and was denoted as YH-*x*.

1.2 Characterization

X-ray powder diffraction (XRD) patterns were recorded using a SHIMADZU XRD-6000 X-ray diffractometer, Ni-filtered $\text{Cu K}\alpha$ radiation, 40 kV and 30 mA. Framework infrared spectra of the calcined samples were obtained on a SHIMADZU FTIR-8400 spectrometer in KBr pellets. Crystal sizes and morphology of the as-synthesized samples were investigated on a JEOL JEM-2010 transmission electron microscopy (TEM) and a HITACHI S4800 scanning electron microscopy coupled with energy dispersive spectroscopy (EDS). ^{29}Si MAS NMR spectra were recorded on a Bruker Avance III 500 spectrometer at resonance frequencies of 99.361 MHz, 50 kHz sample spinning rate, 0.22 μs pulse width, 4 s recycle delay, and 1024 sampling frequency. N_2 adsorption at 77 K was performed in a Micromeritics ASAP2400 gas sorption analyzer to study micro- and mesoporosity in the zeolite crystals. The mesopore size distribution was calculated using Barret–Joyner–Halenda (BJH) pore size model applied to the adsorption branch of the isotherm. The microporous structure was obtained from the *t*-plot analysis of the adsorption branch of the isotherm.

2 Results and discussion

It can be seen from Fig. 1 that after treated by vapor at 90°C for 24 h, the dried gel precursors with $\text{SiO}_2/\text{Al}_2\text{O}_3$ ratios of 4.14–7.25 have been transferred into pure phase Y zeolite with different crystallinity. While XRD patterns of the sample YH-5.18, which is obtained *via* the traditional hydrothermal crystallization from a precursor with the same chemical component as that yielding the sample YS-5.18, not only exhibits the characteristic diffraction peaks ascribed to the FAU topological structure at $2\theta = 6.16^\circ, 10.08^\circ, 15.72^\circ, 20.43^\circ, \text{ and } 23.67^\circ$, but also displays P zeolite characteristic diffraction peaks at $2\theta = 12.46^\circ, 17.66^\circ, 21.67^\circ, 30.84^\circ$. The result indicates that the different synthesis procedures affect the formation of

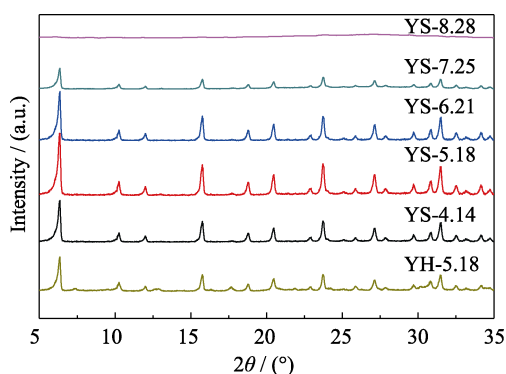


Fig. 1 XRD patterns of the samples

the final products.

As shown in Fig. 2(a-b), the dried gel YP-5.18 exhibits a worm-like morphology, implying the sample an amorphous phase. After being subjected to vapor treatment at 90 °C for 24 h, the worm-like amorphous phase has disappeared and the dried gel has been transferred into crystalline phase (Fig. 2(e-f)). It can be seen from Fig. 2(c-j) that the crystals in all of the final products, such as YS-4.14, YS-5.18, YS-6.21, and YS-7.25, display about 1 μm sphere-like polycrystalline aggregates consisting of loosely aggregating primary crystallites with a size of about 50–300 nm. It can be seen from Fig. 2(d, f, j, i) that the increased Si/Al ratio in the precursors leads to the smaller primary crystals. The weakened characteristic peaks with increased Si/Al ratio in the precursors (Fig. 1) can therefore be partially ascribed to the decreased crystalline size of the primary crystals in the as-synthesized sphere-like Y zeolite polycrystalline aggregates. Higher Si/Al ratio of 8.28 in the precursor gives the final product YS-8.28 the similar worm-like morphology as one of dried gel YP-5.18 (Fig. 2(a-b)). While, as shown in Fig. 3(a-d), a trace of sphere-like polycrystalline aggregate composed of the primary particles with a size of about 100–300 nm can also be observed, indicating that the excessively increased Si/Al ratio in dried gel, for example YP-8.28, mainly yields the amorphous phase, which is in agreement with the result observed by XRD patterns as shown in Fig. 1.

As shown in Fig. 3(i), most of the crystals in the ref-

erence sample YH-5.18 obtained by a traditional hydrothermal synthesis procedure are dense and smooth faujasite with a size of ~ 1000 nm, and some impure crystals, which can be ascribed to P zeolite (Fig. 1), are also observed. A large number of crystals with regular hexagonal platy shape (Fig. 3(e-g)) with size ranging from 1 to 3 μm are found in sample YS-6.21 (Fig. 3(e-g)), and a small quantity of crystals with similar hexagonal platy shape as the one in YH-6.21 can also be observed in sample YS-5.18 as shown in Fig. 3(h).

As shown in Fig. 4, TEM image of the sample YS-5.18 further discovers that the crystals in the samples prepared by the SAC procedure are the polycrystalline aggregates which are composed of loosely aggregating primary crystals with a size of about 50–300 nm, and the polycrystalline aggregates are sticky to each other. Direct evidence for the presence of meso- and macropores with a size of 10–100 nm in diameter is also provided by the TEM image as shown in Fig. 4(a) (red arrow). TEM image (Fig. 4(b)) and the corresponding reversed-phase TEM image (Fig. 4(c)) of the crystal in sample YS-5.18 suggest that some of the sphere-like polycrystalline aggregates are hollow.

FT-IR spectra of the dried gel YP-*x* (dotted line) and the as-synthesized YS-*x* (full line) are shown in Fig. 5. The characteristic vibration bands attributed to zeolite can be observed, although they are not completely identical. The bands at ~ 457 cm^{-1} , ~ 570 cm^{-1} , and ~ 764 cm^{-1} are respectively assigned to the O–T (Si or Al) bending

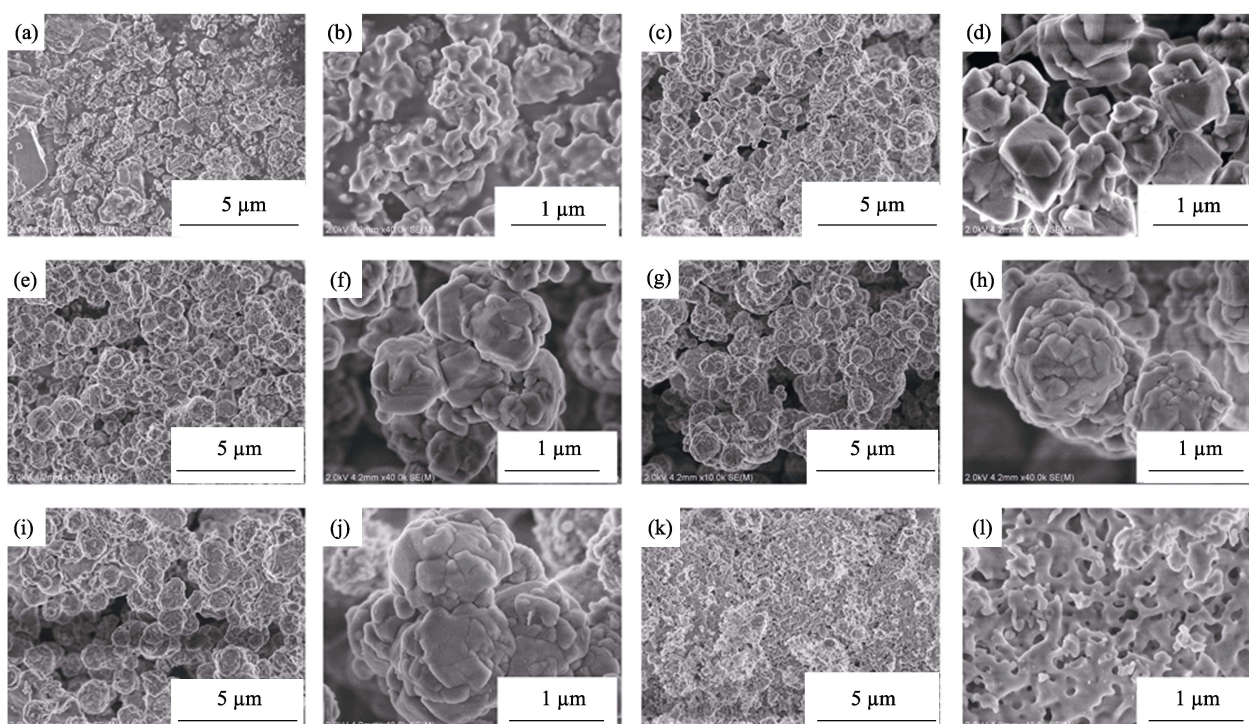


Fig. 2 SEM images of the as-synthesized YS-*x* samples (a, b) YP-5.18; (c, d) YS-4.14; (e, f) YS-5.18; (g, h) YS-6.21; (i, j) YS-7.25; (k, l) YS-8.28

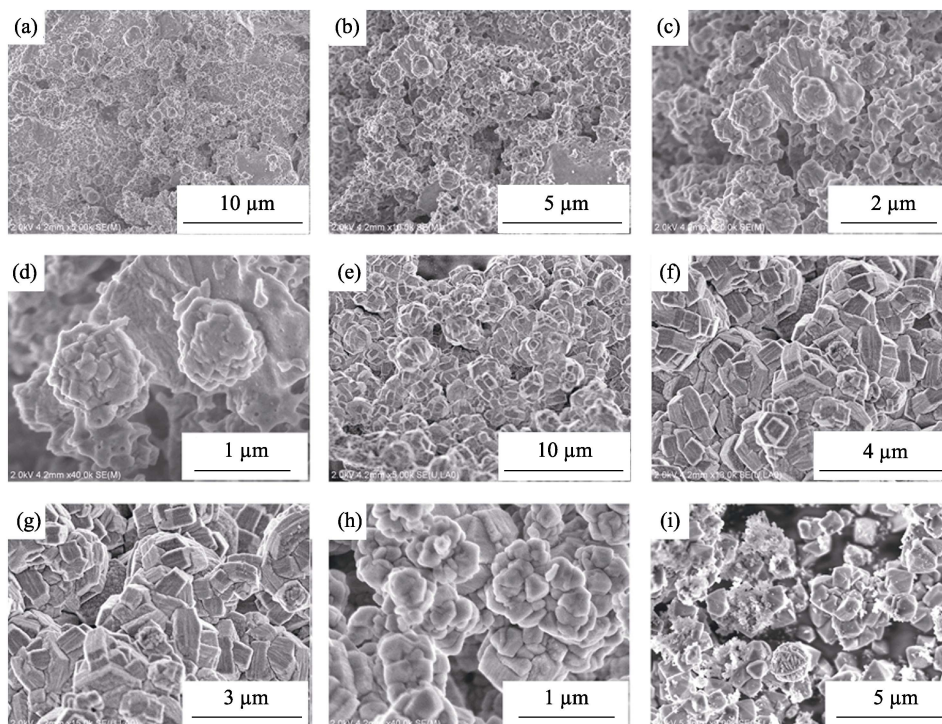


Fig. 3 SEM images of the as-synthesized Y zeolite yielding from the gel precursor with different Si/Al ratio (a-d) YS-8.28; (e-g) YS-6.21; (h) YS-5.18; (i) YH-5.18

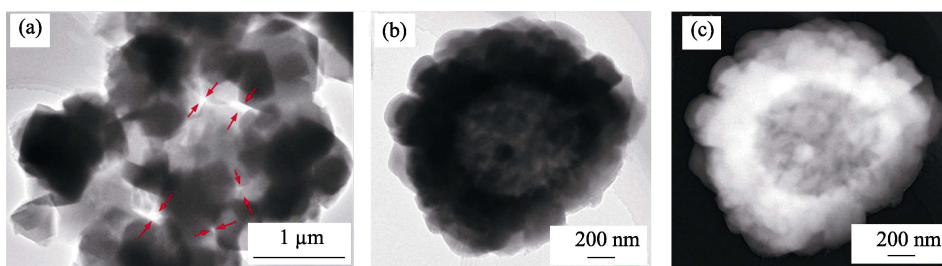


Fig. 4 TEM image of YS-5.18 (a), TEM image (b) and the corresponding reversed-phase TEM image (c)

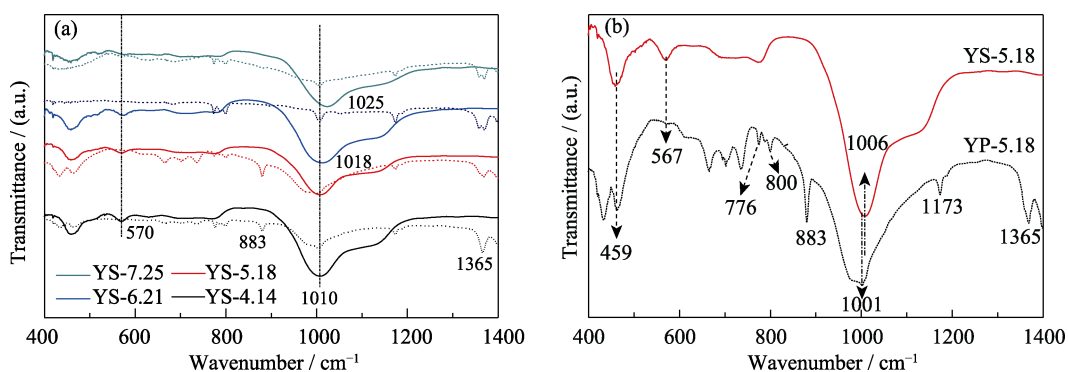


Fig. 5 FT-IR spectra of the samples

(a) YS-*x* (solid curves) and the corresponding dried gel precursors YP-*x* (dotted curves); (b) YS-5.18 and YP-5.18

vibrations, the double ring external linkage vibrations, and the external linkage symmetrical stretching vibrations.

For Y zeolite, the band at around 1010–1025 cm^{-1} is ascribed to the internal tetrahedral asymmetrical stretching vibration. The vibration bands between 1000 cm^{-1} and 1100 cm^{-1} are often used to identify the Si/Al ratio of

zeolite framework. The anti-symmetric stretching vibration bands corresponding to YS-4.14, YS-5.18, YS-6.21, and YS-7.25 are respectively located at 1010, 1010, 1018 and 1025 cm^{-1} , implying the as-synthesized samples may have an increased framework Si/Al ratio^[23]. As shown in Fig. 6, EDS analytical result suggests that the

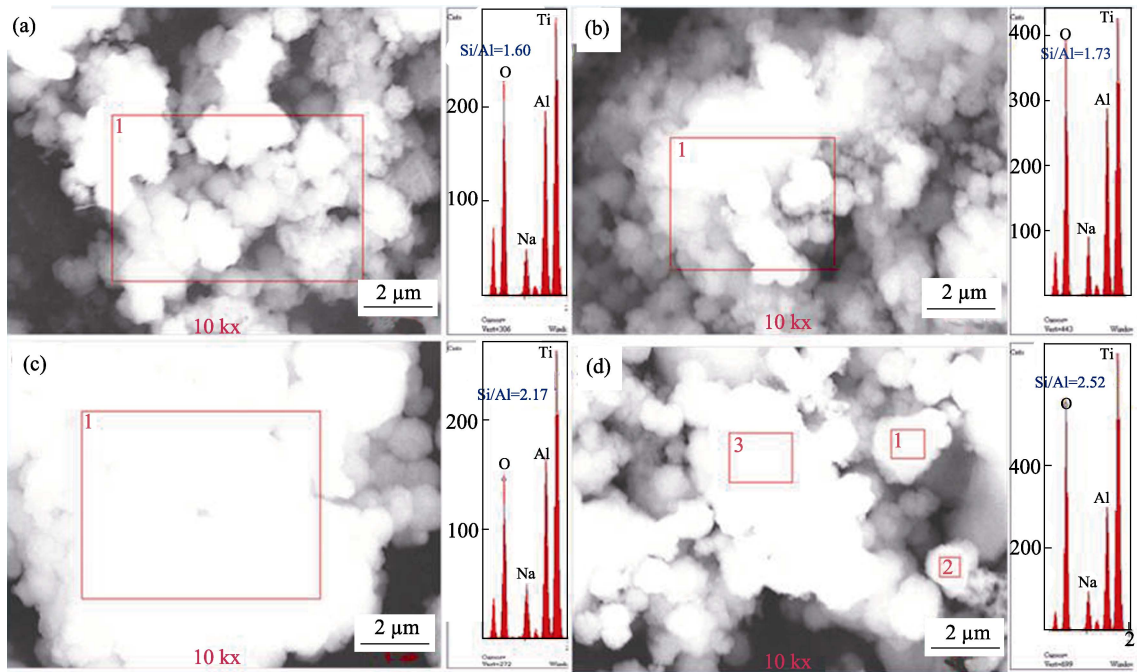


Fig. 6 SEM images and EDS analysis of the as-synthesized Y zeolite yielding from gel precursor with different Si/Al ratio (a) YS-4.14; (b) YS-5.18; (c) YS-6.21; (d) YS-7.25

surface $\text{SiO}_2/\text{Al}_2\text{O}_3$ ratio in the final products are 3.20 for YS-4.14, 3.46 for YS-5.18, 4.34 for YS-6.21, and 5.04 for YS-7.25. The variation tendency generally agrees with the result detected by FT-IR. As shown in Fig. 5(a, b), the dotted curves represent FT-IR spectra of the corresponding dried gel YP-*x*. Two keen-edged peaks, which are respectively located at 883 cm^{-1} and 1365 cm^{-1} , can be ascribed to the existence of the amorphous silicon and aluminum species^[24]. The band at $\sim 570\text{ cm}^{-1}$ to the double ring external linkage vibrations, and the band at about 1000 cm^{-1} ascribed to the anti-symmetric stretching vibrations band are obviously observed, implying that partial silicon or/and aluminum species have been transferred into primary or/and secondary building units^[25]. As shown in Fig. 5(b), the comparison result of the FT-IR spectra between YP-5.18 and YS-5.18 clearly suggests that double ring external linkage vibrations, and the anti-symmetric stretching vibrations are obviously observed in dried gel YP-5.18, and the location of these vibrations is completely identical to that in YS-5.18. The above mentioned results imply that the primary or/and secondary building units have been formed during the preparation of the dried gel despite of exhibiting the worm-like amorphous morphology (Fig. 2(a, b)).

Figure 7(a) and (b) are ^{29}Si MAS NMR spectra of sample YS-5.18 and the corresponding dried gel YP-5.18, respectively. The resonances at $\delta = -108 \sim -105$ are assigned to Si (4Si, 0Al) sites, and those $\delta = -105 \sim -95$ are assigned to Si (3Si, 1Al) sites; moreover, those at $\delta = -95 \sim -92$, $-92 \sim -86$, and $-86 \sim -80$, are respectively as-

signed to the Si (2Si, 2Al), Si (1Si, 3Al), and Si (0Si, 4Al)^[26]. The calculated framework Si/Al ratio of sample YS-5.18 is about 1.65 (Table 1), which is slightly lower than 1.73 detected by EDS. It can be seen from Fig. 7(b) that the resonances assigned to Si (0Si, 4Al), Si (1Si, 3Al) and Si (2Si, 2Al) sites can be obviously observed in dried gel YP-5.18, indicating that the primary zeolite

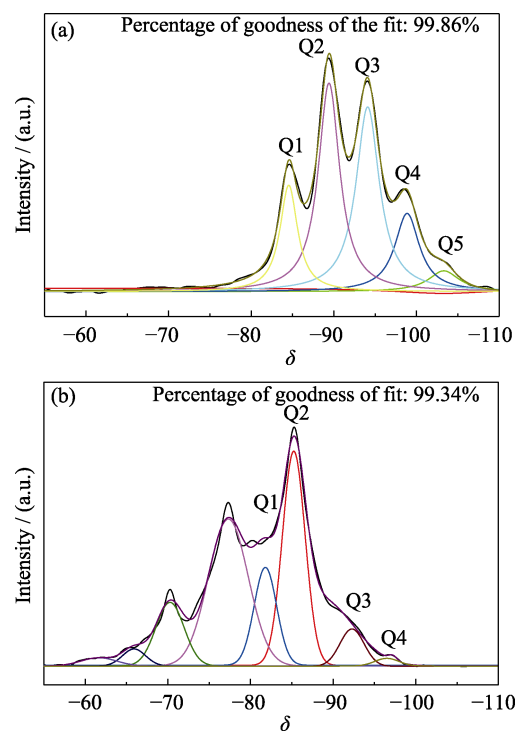


Fig. 7 ^{29}Si MAS NMR spectra (a) YS-5.18; (b) YP-5.18

framework has been practically formed in dried gel yielded from the gel mixture after treated at 60 °C for 24 h. The calculated framework Si/Al ratio of dried gel YP-5.18 is about 1.27 (Table 1), which is rather lower than 1.65 of the final product YS-5.18. The aforementioned results suggest that the primary zeolite framework formed during the preparation of the dried gel has a rather lower Si/Al ratio as compared with the one in final products. The calculated framework Si/Al ratio and the different aluminium coordination are shown in Table 1. It can be inferred that the primary zeolite framework formed during preparing dried gel is rich in Al-, and Si-species entering the zeolite framework fall behind the Al-species. Combining with the FT-IR result as shown in Fig. 5, it can be further deduced that some building units or minicrystals with primary zeolite framework, which are not yet detected by XRD or TEM because of very small spatial scale, have been really formed during the preparation of the dried gel precursors.

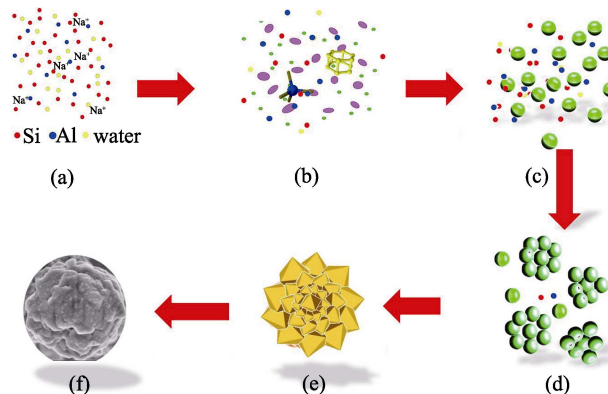
Table 1 Quantification by ^{29}Si MAS NMR for sample YS-5.18 and the corresponding dried gel precursor YP-5.18

Sample	*Q1%	Q2%	Q3%	Q4%	Q5%	Si/Al
YS-5.18	18.2	30.8	31.4	13.9	5.7	1.65
YP-5.18	19.7	36.5	7.3	1.3	0	1.27

*: Q1, Q2, Q3, Q4, and Q5 respectively represent Si (0Si, 4Al), Si (1Si, 3Al), Si (2Si, 2Al), Si (3Si, 1Al) and Si (4Si, 0Al) sites

The building units or crystallites with the primary zeolite framework yielded during the preparation of the dried gel play an important role in the formation of the hierarchical sphere-like Y zeolite consisting of nanocrystals. The formed building units or the primary crystallites in the dried gel not only offers the target product a fast nucleation, but also plays a key role in guaranteeing the precursor to be transferred into the pure phase FAU zeolites structure. During SAC procedure, these building units or crystallite with primary zeolite framework in the dried gel induced a burst in nucleation rate^[8], and nano-sized zeolite crystals were created that subsequently self-assembly formed sphere-like polycrystalline Y aggregates^[8, 11].

Indeed, despite very complex for the mechanisms of zeolite growth and nucleation, it is very obvious that a high ratio of nucleation relative to growth is in favor of the formation of nanocrystals. The crystallization mechanism of the sphere-like Y consisting of loosely aggregating nanocrystallites is interpreted in Scheme 1. During preparation of dried gel, primary or/and secondary building units^[25], or even crystallite with primary zeolite framework (as detected by FT-IR and ^{29}Si NMR) are



Scheme 1 Schematic representation of the process for the formation of the sphere-like hierarchical Y zeolite composed of the loosely aggregating nanocrystallites

induced and bred (Scheme 1(a)→(b)). During SAC process, a vast amount of crystal nucleus, which are evolved from the building units or crystallite, form in an extremely short time, and nano-sized zeolite crystals are therefore created (Scheme 1(b)→(c)). The single nanocrystals are unstable, they are inclined to self-assemble into sphere-like polycrystalline aggregates so as to decrease the high surface free energy (Scheme 1(c)→(d)). The nanocrystals outer the “sphere” conduct an epitaxy growth because of the confined space effect (Scheme 1(d)→(e)); meanwhile, the nanocrystals inner the “sphere” may be consumed by the oriented growth crystals outer the “sphere” in the manner of the “Ostwald ripening process”, that leads to forming the hollow polycrystalline Y zeolite spheres.

Fig. 8 is N_2 adsorption-desorption isotherms of the as-synthesized YS-*x* zeolite samples obtained from the dried gel precursors with a different $\text{SiO}_2/\text{Al}_2\text{O}_3$ ratio. The adsorption-desorption of nitrogen on sample YH-5.18 is a type-I isotherm, indicating the presence of micropores only. However, larger hysteresis loops occur in the adsorption-desorption isotherms of the YS-4.14, YS-5.18, YS-6.21 and YS-7.25, indicating the presence of mesopores in the samples obtained by SAC procedure. Combining with the results observed in SEM images mentioned in Fig. 2 and TEM image shown in Fig. 4, the larger hysteresis loops occurring in the isotherms should therefore be attributed to capillary condensation in open mesopores or macropores obtained by filling the primary nanocrystals or polycrystalline aggregates interparticle spaces^[7-8]. As shown in Fig. 8(b), the pore size distribution of the YS-4.14, YS-5.18, and YS-6.21 obtained from the adsorption branch of the isotherm illustrates the existence of a meso- and macropore structure with pore sizes 4–100 nm, which is in good agreement with the results observed in SEM and TEM images. However, the BJH pore size distribution derived from the adsorption branch

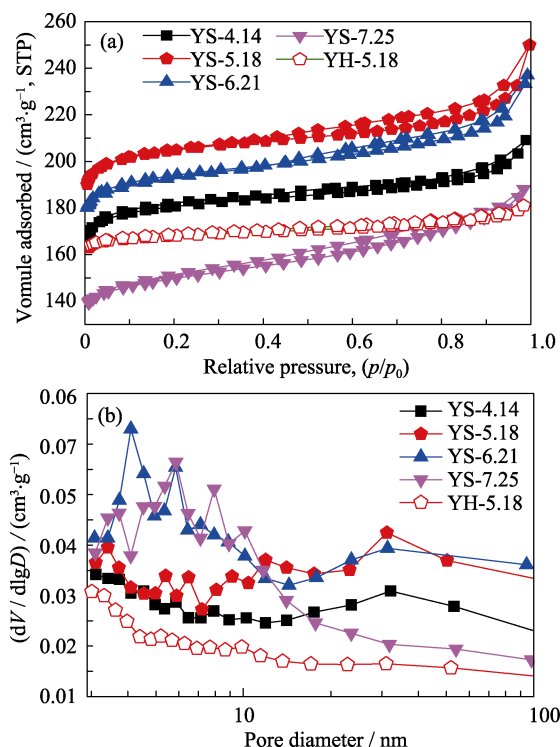


Fig. 8 N_2 adsorption-desorption isotherms (a) and pore size distribution curves (b)

of the isotherm does not show the similar distribution in the YH-5.18.

It can be seen from Table 2 that the external surface areas of the as-synthesized hierarchical Y are 41–51 m^2/g , which is more than 2 times as much as the 21 m^2/g of the reference YH-5.18 zeolite obtained by traditional hydrothermal procedure. The elevated external surface areas can be attributed to the nanocrystallization of primary Y crystalline grains in the sphere-like hierarchical Y. Table 2 also illustrates that the micropore surface area and volume of the sphere-like Y are lower varying degree than 714 m^2/g and 0.27 cm^3/g of the reference YH-5.18, respectively because of the deteriorated ordering of three-dimensional network of the primary nanocrystals. The aforementioned results indicate that a hierarchical pore system has been introduced into the as-synthesized Y sample, which owns the regular micropores of FAU zeolite structure, and a meso- and macroporous system resulting from the interparticle spaces of nano-sized primary or polycrystalline aggregating Y crystals.

Table 2 Physical structural properties of the samples

Samples	S_{BET} /($m^2 \cdot g^{-1}$)	S_{mic} /($m^2 \cdot g^{-1}$)	S_{ext} /($m^2 \cdot g^{-1}$)	V_{mic} /($cm^3 \cdot g^{-1}$)	V_{total} /($cm^3 \cdot g^{-1}$)
YS-4.14	739	698	41	0.26	0.34
YS-5.18	837	792	46	0.30	0.40
YS-6.21	791	740	51	0.28	0.38
YS-7.25	730	570	160	0.19	0.31
YH-5.18	735	714	21	0.27	0.35

3 Conclusions

Sphere-like hierarchical Y zeolite polycrystalline aggregates consisting of primary crystals were synthesized by a “Steam-Assisted Conversion (SAC)” procedure. Primary or/and subprime building units or crystallites with primary zeolite framework were verified to be created during preparing the dried gel, and the created building units or crystallites induced a burst in nucleation rate, and primary nano-sized zeolite crystals were created that subsequently self-assembly formed sphere-like polycrystalline Y aggregates. The loosely aggregating nanocrystallites offer the as-synthesized samples a larger mesopore volume and external surface areas at the cost of less sacrificed micropore volume and micropore area.

References:

- [1] CHEN W Z, HAN D M, SUN X H, *et al.* Studies on the preliminary cracking of heavy oils: contributions of various factors. *Fuel*, 2013, **106**(2): 498–504.
- [2] CHOUDHARY T V. Structure-reactivity-mechanistic considerations in heavy oil desulfurization. *Industrial & Engineering Chemistry Research*, 2007, **46**(25): 8363–8370.
- [3] MITCHELL S, BOLTZ M, LIU J X, *et al.* Engineering of zsm-5 zeolite crystals for enhanced lifetime in the production of light olefins via 2-methyl-2-butene cracking. *Catalysis Science & Technology*, 2017, **7**: 64–74.
- [4] XU D D, MA Y H, JING Z F, *et al.* π - π interaction of aromatic groups in amphiphilic molecules directing for single-crystalline mesostructured zeolite nanosheets. *Nature Communications*, 2014, **5**: 4262–4270.
- [5] CHOI M, CHO H S, SRIVASTAVA R, *et al.* Amphiphilic organosilane-directed synthesis of crystalline zeolite with tunable mesoporosity. *Nature Materials*, 2006, **5**(9): 718–723.
- [6] GROEN J C, BACH T, ZIESE U, *et al.* Creation of hollow zeolite architectures by controlled desilication of Al-zoned zsm-5 crystals. *Journal of the American Chemical Society*, 2005, **127**(31): 10792–10793.
- [7] ZHANG J L, PENG C, YAN H Y, *et al.* Synthesis of hierarchical zeolite beta with low organic template content via the steam-assisted conversion method. *Chemical Engineering Journal*, 2016, **291**: 82–93.
- [8] MÖLER K, YILMAZ B, JACUBINAS R M, *et al.* One-step synthesis of hierarchical zeolite beta via network formation of uniform nanocrystals. *Journal of the American Chemical Society*, 2011, **133**(14): 5284–5295.
- [9] VALTCHEV V, BALANZAT E, MAVRODINOVA V, *et al.* High energy ion irradiation-induced ordered macropores in zeolite crystals. *Journal of the American Chemical Society*, 2011, **133**(46): 18950–18956.
- [10] XU L, JI X Y, LI S H, *et al.* Self-assembly of cetyltrimethylammonium bromide and lamellar zeolite precursor for the preparation of hierarchical MWW zeolite. *Chemistry of Materials*, 2016, **28**(12): 4512–4521.
- [11] ZHAO Y, ZHANG H B, WANG P C, *et al.* Tailoring the morphology of MTW zeolite mesocrystals: intertwined classical/nonclassical crystallization. *Chemistry of Materials*, 2017, **29**(8): 3387–3396.

- [12] WINTER D A M D, MEIRER F, WECKHUYSEN B M. FIB-SEM tomography probes the mesoscale pore space of an individual catalytic cracking particle. *ACS Catalysis*, 2016, **6(5)**: 3158–3167.
- [13] KORTUNOV P, VASENKOV S, KARGER J, *et al.* The role of mesopores in intracrystalline transport in usy zeolite: PFG NMR diffusion study on various length scales. *Journal of the American Chemical Society*, 2005, **127(37)**: 13055–13059.
- [14] XUE C F, XU T T, ZHENG J J, *et al.* Silicalite-1 monolith with vertically aligned mesopores templated from carbon nanotube array. *Materials Letters*, 2015, **154**: 55–59.
- [15] ZHU J, ZHU Y H, ZHU L K, *et al.* Highly mesoporous single-crystalline zeolite beta synthesized using a nonsurfactant cationic polymer as a dual-function template. *Journal of the American Chemical Society*, 2014, **136(6)**: 2503–2510.
- [16] ZHU H B, LIU Z C, WANG Y D, *et al.* Nanosized CaCO₃ as hard template for creation of intracrystal pores within silicalite-1 crystal. *Chemistry of Materials*, 2008, **20(3)**: 1134–1139.
- [17] XU W Y, DONG J X, LI J P, *et al.* A novel method for the preparation of zeolite ZSM-5. *Journal of the Chemical Society, Chemical Communications*, 1990, **10(10)**: 755–756.
- [18] MATSUKATA M, OGURA M, OSAKI T, *et al.* Conversion of dry gel to microporous crystals in gas phase. *Topics in Catalysis*, 1999, **9(1/2)**: 77–92.
- [19] HU D, XIA Q H, LU X H, *et al.* Synthesis of ultrafine zeolites by dry-gel conversion without any organic additive. *Materials Research Bulletin*, 2008, **43(12)**: 3553–3561.
- [20] MATSUKATA M, OGURA M, OSAKI T, *et al.* Quantitative analyses for TEA⁺ and Na⁺ contents in zeolite beta with a wide range of Si/Al ratio. *Microporous & Mesoporous Materials*, 2001, **48(1)**: 23–29.
- [21] ALFARO S, ARRUEBO M, CORONAS J, *et al.* Preparation of MFI type tubular membranes by steam-assisted crystallization. *Microporous & Mesoporous Materials*, 2001, **50(2/3)**: 195–200.
- [22] ZHANG J, BAI S, CHEN Z W, *et al.* Core-shell zeolite Y with ant-nest like hollow interior constructed by amino acids and enhanced catalytic activity. *Journal of Materials Chemistry A*, 2017, **5(39)**: 20757–20764.
- [23] ZHANG X W, GUO Q, QIN B, *et al.* Structural features of binary microporous zeolite composite Y-beta and its hydrocracking performance. *Catalysis Today*, 2010, **149(1)**: 212–217.
- [24] MORSLI A, DRIOLE M F, CACCIAGUERRA T, *et al.* Microporosity of the amorphous aluminosilicate precursors of zeolites: the case of the gels of synthesis of mordenite. *Microporous & Mesoporous Materials*, 2007, **104(1/2/3)**: 209–216.
- [25] RANI V R, SINGH R, PRAMATHA P A, *et al.* Existence of colloidal primitive building units exhibiting memory effects in zeolite growth compositions. *Journal of Physical Chemistry B*, 2004, **108(52)**: 20465–20470.
- [26] DEKA J, SATYANARAYANA L, KARUNAKAR G V, *et al.* Chiral modification of copper exchanged zeolite-Y with cinchonidine and its application in the asymmetric Henry reaction. *Dalton Transactions*, 2015, **44(48)**: 20949–20963.

“蒸汽相转化”法制备球形多级 Y 沸石

杜艳泽^{1,2}, 杨晓娜¹, 宁伟巍¹, 孔庆岚¹,
秦波², 郑家军¹, 李文林¹, 李瑞丰¹

(1. 太原理工大学 能源化工与催化研究中心, 煤科学与技术教育部与山西省重点实验室, 太原 030024; 2. 中国石油化工集团 大连石油化工研究院, 大连 116045)

摘要: 本文采用“蒸汽相转化”法合成了球形多级 Y 沸石。采用 X 射线衍射(XRD), 扫描电镜(SEM), 透射电子显微镜(TEM), N₂吸附-脱附, 固态核磁共振(NMR)谱和傅里叶变换红外(IR)光谱等表征手段对制备材料的结构性能进行了表征。SEM 观察结果表明合成的 Y 型沸石是由尺寸为 50~300 nm 的初级晶粒组成的球形多晶聚集体, 透射电镜观察结果表明多晶聚集体为空心 Y 型沸石。通过分析 FT-IR, ²⁹Si NMR, SEM 和 TEM 等表征结果, 提出了空心球形 Y 沸石的形成机理。

关键词: 多级孔; 多晶聚集体; 空心球; “蒸汽相转化”法

中图分类号: TQ174 文献标识码: A